

# Water Resources Research®

## RESEARCH ARTICLE

10.1029/2021WR031307

### Key Points:

- Hysteresis-based results show higher degradation risk and slower rehabilitation when irrigating with saline and sodic treated wastewater
- Actual degradation risk results from dynamic interplay between a soil's susceptibility to degradation and its ability to rehabilitate
- SOTE model is first to consider effects of hysteresis on changes in saturated soil hydraulic conductivity under saline and sodic conditions

### Supporting Information:

Supporting Information may be found in the online version of this article.

### Correspondence to:

Y. Mau,  
[yair.mau@mail.huji.ac.il](mailto:yair.mau@mail.huji.ac.il)

### Citation:

Kramer, I., Bayer, Y., & Mau, Y. (2022). The sustainability of treated wastewater irrigation: The impact of hysteresis on saturated soil hydraulic conductivity. *Water Resources Research*, 58, e2021WR031307. <https://doi.org/10.1029/2021WR031307>

Received 27 SEP 2021

Accepted 13 FEB 2022

## The Sustainability of Treated Wastewater Irrigation: The Impact of Hysteresis on Saturated Soil Hydraulic Conductivity

Isaac Kramer<sup>1</sup> , Yuval Bayer<sup>1</sup> , and Yair Mau<sup>1</sup> 

<sup>1</sup>Institute of Environmental Sciences, The Robert H. Smith Faculty of Agriculture, Food and Environment, Hebrew University of Jerusalem, Rehovot, Israel

**Abstract** Models for the effect of salinity and sodicity on saturated soil hydraulic conductivity,  $K_s$ , have yet to consider hysteresis. Ignoring hysteresis limits our ability to assess the risk posed by irrigation with saline and sodic water, such as treated wastewater (TWW). We introduce SOTE 2.0, the first model to consider hysteresis in  $K_s$ , as driven by different climate and irrigation regimes. The new model integrates the SOTE 1.0 model for salinity and sodicity dynamics with a model for the effect of saline and sodic water on  $K_s$  that explicitly includes hysteresis. SOTE 2.0 is used to demonstrate how hysteresis significantly alters our understanding of degradation and rehabilitation. SOTE 2.0 relies on weight functions to highlight soil-specific differences in degradation and rehabilitation patterns. While TWW irrigation can be crucial to mitigating water scarcity, simulations show that salinity and sodicity have the potential to irreversibly damage soil structure, as measured by declines in  $K_s$ . Compared to the McNeal model used by Hydrus and others, SOTE predicts up to 50% degradation risk in settings where the McNeal model predicts none. The SOTE model also predicts slower rehabilitation: up to 100 days, compared to 0 days when using the McNeal model. Results highlight the difference between susceptibility and risk, showing that the probability of degradation is not solely dependent on initial susceptibility to degradation. To fully characterize a soil, we must also know its propensity to rehabilitation.

**Plain Language Summary** Models for the assessment of how irrigation water affects soils have always assumed that “what goes down must come back up.” While significant research has investigated how low-quality irrigation water causes soil degradation, almost none has studied the process in reverse: how easily can a degraded soil be rehabilitated? We use a mathematical model to demonstrate that this question is crucial to understanding the risk of irrigation with treated wastewater (TWW). TWW irrigation—increasingly common in water-scarce regions—can cause irreversible damage to soils, if the water is saline and sodic. In this paper, we model degradation and rehabilitation as separate processes, as experimental evidence indicates they should be. The mathematical framework introduced here is capable of reflecting the fact that rehabilitation and degradation likely occur on much different time scales, with changes in soil structure dependent on a soil's history of degradation and rehabilitation. When using the new model, risk of degradation moves from 0% to over 50%. Likewise, our model estimates that the cost (time and resources) of rehabilitation are likely to increase. More accurate models facilitate smarter decision making, giving us the ability to continue irrigation with TWW in ways that minimize long-term risk of soil degradation.

## 1. Introduction

Irrigation with treated wastewater (TWW) presents both opportunity and risk. In many cases, using TWW is an economically advantageous way of sustaining agricultural production in areas where freshwater resources are limited (Assouline et al., 2015; Bixio et al., 2006; Dery et al., 2019; Jaramillo & Restrepo, 2017; Winpenny et al., 2010). On the other hand, the salinity and sodicity content of TWW is often higher than that of freshwater, and this can imperil soils (Assouline et al., 2015; Ben-Gal et al., 2006; Hillel, 2000). Salinity and sodicity induced land degradation is already an acute concern in arid and semiarid regions (Dregne & Chou, 1992; Práválie et al., 2021; Safriel et al., 2005), with growing populations and changing precipitation patterns expected to intensify water scarcity (Assouline et al., 2015; Safriel et al., 2005), which is likely to increase reliance on marginal quality water sources for agricultural production. Adding to the severity of the issue, land degradation itself can be a driver of climate change, leading to a net carbon release (Olsson et al., 2019).

In this article, we focus on relative saturated hydraulic conductivity (relative  $K_s$ ) as a lead indicator of land degradation. Relative  $K_s$  compares the present value of soil  $K_s$  to the original value, and thus represents the degree to which a soil has experienced a decline in hydraulic conductivity. Because it represents the rate at which the soil is able to transmit water,  $K_s$  can be considered a proxy for numerous soil characteristics, including soil structure, porosity, and water retention (Hillel, 1998). Easy movement of water, air, and solutes through the soil is crucial to healthy plant growth, and therefore declines in relative  $K_s$  are a reliable signal of potential land degradation.

The primary mechanism through which saline and sodic TWW threatens hydraulic conductivity is the breakdown of soil aggregates (Assouline & Narkis, 2011; McNeal & Coleman, 1966; Shainberg & Singer, 2011; Yaron & Thomas, 1968). This tends to occur when the relative concentration of sodium ions in a soil's cation exchange complex is high, but the overall salinity concentration is low (Bresler et al., 1982; Levy et al., 2005; Shainberg & Letey, 1984, 1992). These conditions—common when irrigation with saline TWW is followed by precipitation—result in a weakening of the bonds between soil particles, which can cause clay swelling, clay dispersion, and slaking (Bresler et al., 1982; Levy et al., 2005; Shainberg & Letey, 1984, 1992). When this occurs, the movement of water and air through the soil is restricted, presenting a direct threat to plant growth and agricultural output (Assouline & Narkis, 2011, 2013; Bardhan et al., 2016; Läuchli & Grattan, 2011; Shainberg & Singer, 2011). Rehabilitation of degraded soils, meanwhile, is often technically difficult, resource intensive, and slow, in addition to being expensive (Gharaibeh et al., 2011; Oster, 1993; Qadir et al., 2001).

This degradation is not always completely reversible, with experimental evidence indicating that changes in  $K_s$  as a result of salinity are characterized by hysteresis (Adeyemo et al., 2022; Dane & Klute, 1977; Kramer et al., 2021). That is to say, while  $K_s$  can be expected to decline under saline and sodic conditions, results do not suggest that an improvement in chemical conditions will cause  $K_s$  to rise at the same rate that it declined. Rather, the degree to which changes in  $K_s$  are reversible is likely soil specific, with initial results challenging the expectation that higher clay contents lead to lower degrees of reversibility (Adeyemo et al., 2022), though the degree to which this is true can be expected to vary significantly depending on the clay mineralogy of a soil.

Despite the myriad risks that irrigation with saline and sodic TWW pose to sustainable food production, existing tools for managing these dangers do not account for any hysteresis in  $K_s$ . On the contrary, when predicting  $K_s$  values, models for the effect of irrigation practices and climate regimes on  $K_s$  (Kramer & Mau, 2020; Šimůnek et al., 2013; van der Zee et al., 2014) rely on experimental knowledge of the degradation process only. Specifically, they integrate empirical models (Ezlit et al., 2013; McNeal, 1968) that were developed based on soil column experiments in which reductions in  $K_s$  were measured as input water of changing chemical composition was applied. The dynamic models then assume that there are no differences between the degradation and rehabilitation processes, and use the empirical models to predict increases, as well as decreases, in  $K_s$ . In doing so, these models neglect the fact that rehabilitation and degradation are very different processes and that reversing the series of chemical conditions that led to a decline in  $K_s$  is unlikely to lead to a subsequent and equal rise in  $K_s$ . Failure to differentiate between the degradation and rehabilitation, therefore, has the potential to introduce significant error when analyzing the sustainability of irrigation with marginal quality water, such as TWW. Likewise, this simplification may hinder our ability to estimate the time and resources required for rehabilitation. It is for these reasons that development of models that can improve the management of saline and sodic water resources is considered a research priority (Hopmans et al., 2021).

Our objective in this paper is to address this gap, by developing a model for the dynamics of soil salinity and sodicity, which is explicitly capable of considering hysteresis in  $K_s$ . We begin in Section 2, by integrating SOTE 1.0 (Kramer & Mau, 2020)—a model for the dynamics of soil water content, salinity concentration, and relative sodicity—with a recently introduced module for irreversible changes in  $K_s$  (Kramer et al., 2021). In contrast to the models noted earlier, the framework developed by Kramer et al. (2021) is the only one that includes hysteresis in  $K_s$  under changing water chemistry. We then use the integrated model, called SOTE 2.0, to highlight the clear effects that hysteresis has on  $K_s$  dynamics, when modeling both degradation and rehabilitation scenarios (Section 3). Finally, we perform a sensitivity analysis to identify the parameters that most influence the model's output, and to evaluate the robustness of the results under uncertain input conditions.

## 2. Modeling Framework

This section introduces SOTE 2.0—a model for how salinity and sodicity, as driven by irrigation practices and climate conditions, affect soil  $K_s$ , explicitly accounting for both hysteresis and soil-specific differences. We open with a short discussion of SOTE 2.0's underlying components: SOTE 1.0 and the Preisach framework for changes in  $K_s$ . This section also discusses the soil-specific parameters used throughout this paper, and comments on the general framework used in the simulations that follow. To differentiate between SOTE 2.0 and the original SOTE 1.0, we use version numbers where any ambiguity is possible. Any references to SOTE that do not include a version number refer to SOTE 2.0.

### 2.1. SOTE 1.0

SOTE 1.0 (Kramer & Mau, 2020) focuses on the dynamics of three state variables: (i) Relative soil water content,  $s$  (dimensionless); (ii) Salinity, that is, the electrolyte concentration of the soil water,  $C_s$  ( $\text{mmol}_c \text{L}^{-1}$ ); and (iii) Sodidity, that is, the fraction of sodium ions in the soil's exchange complex ( $E_x$ , dimensionless). The system is driven by irrigation (chemical composition and application rates) and climate (precipitation and evapotranspiration rates). With a focus on ease of analysis over strict precision, the model averages soil properties over both the horizontal and vertical directions, such that there are no explicit spatial dimensions. Likewise, the chemical composition of the drainage water is taken to be equal to that of the soil water itself, assuming complete mixing in the root zone. Finally, SOTE 1.0 focuses on only two cations,  $\text{Na}^+$  and  $\text{Ca}^{2+}$ . This commonly employed practice (Bolt, 1967; Bresler et al., 1982; Mau & Porporato, 2015; van der Zee et al., 2014) allows for emphasis on the differing effects monovalent (associated with degradation) and divalent (associated with aggregate stability) cations have on soil structure. SOTE 1.0 was successfully evaluated against a 4-year lysimeter experiment (Kramer & Mau, 2020), driven by varying irrigation water compositions during the summer, and by precipitation during the winter and against field data from the Sangong River watershed (SRW) of northwestern China (Yin et al., 2021).

The contrasting effects that  $\text{Na}^+$  and  $\text{Ca}^{2+}$  have on soil structure is a major focus of SOTE 1.0, with changes in the chemical composition of the soil water causing feedback with saturated soil hydraulic conductivity,  $K_s$ . In SOTE 1.0, this feedback is accounted for by integrating the Ezlit et al. (2013) model for the effect of salinity and sodicity on  $K_s$ . Similar to earlier models (McNeal, 1968), Ezlit et al. (2013) is based on the results of soil column experiments in which degradation of  $K_s$  was measured following the application of water of varying chemical composition. The Ezlit et al. (2013) model is an improvement, since it considers soil-specific differences in how salinity and sodicity affect  $K_s$ . Neither Ezlit et al. (2013) nor McNeal (1968), however, consider the effect of partial reversibility on changes in  $K_s$ , that is, both assume there are no differences between the process of rehabilitation and degradation. As such, the dynamics in SOTE 1.0 are also incapable of considering the effects of hysteresis.

### 2.2. The Preisach Framework for Changes in $K_s$

In SOTE 2.0, the Ezlit et al. (2013) equations are exchanged in favor of a module capable of accounting for hysteresis in  $K_s$ . Specifically, SOTE 2.0 integrates the Preisach framework for changes in  $K_s$ , as presented in Kramer et al. (2021), which is unique in its ability to consider how a soil's history of degradation and rehabilitation will affect its future state. The Preisach framework is founded on the idea of hysterons, elementary switches that can be turned “on” and “off” according to predefined thresholds. Kramer et al. (2021) adapted the original framework so that its inputs are salinity concentration ( $C_s$ ) and sodium adsorption ratio (SAR), while  $K_s$  is the output. While SOTE 1.0, like all other existing models, is “memoryless,” that is, future states of the system depend only the present state, the dynamics prescribed by SOTE 2.0 depend on the whole of salinization and sodification. This is an important, and as we will show, necessary step toward modeling realism.

A major advantage of the Preisach framework is that it can produce hysteresis curves of any shape. This is achieved through the use of experimentally determined “weight functions,” which make it possible to account for soil-specific differences in both the shape of the hysteresis curves, as well as patterns of degradation and rehabilitation. Readers unfamiliar with the Preisach framework are encouraged to use the interactive widgets available at <http://github.com/yairmau/hysteresis-python>, which demonstrate how changing input values, together with different weight functions, can produce various types of hysteresis curves. The Preisach framework can also be easily modified so that the hysteresis curves demonstrate only partial recovery, instead of a full loop.

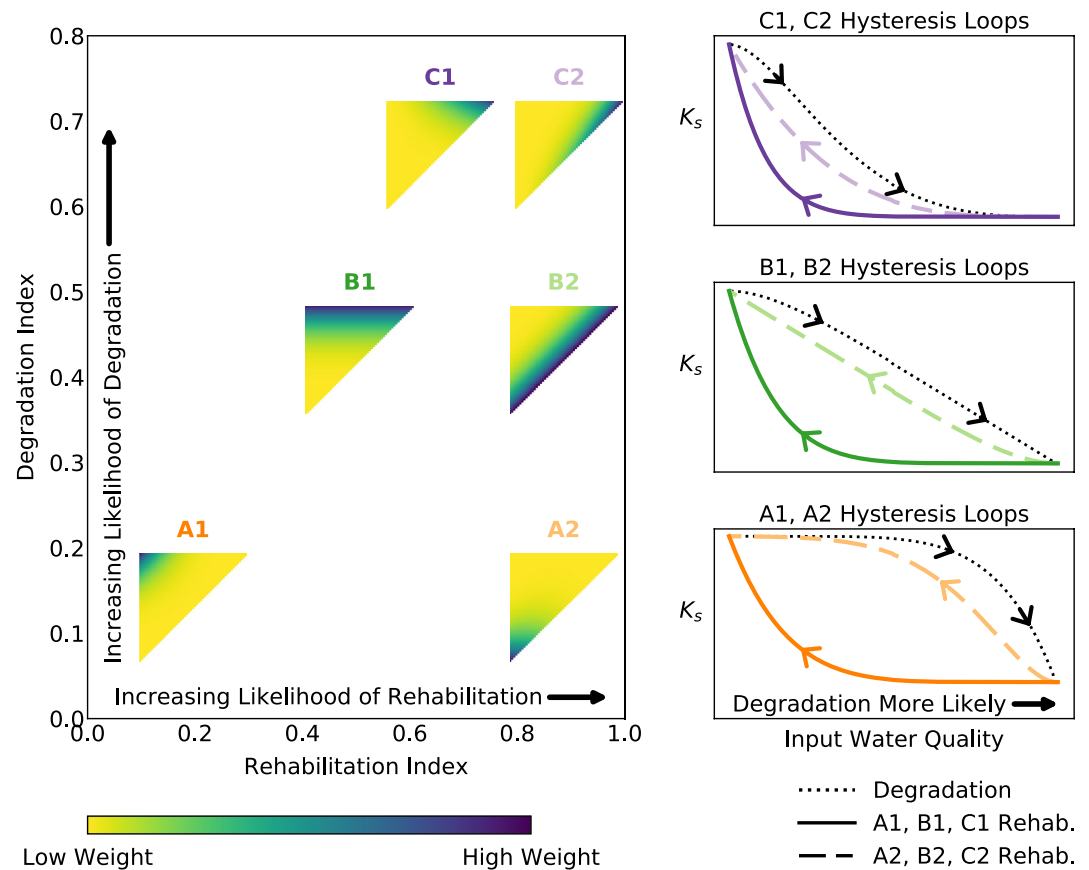


**Figure 1.** Weight functions are the key to producing differently shaped hysteresis curves. Left panel shows weight functions used in this paper according to their degradation index (susceptibility to degradation) and rehabilitation index (propensity to rehabilitation). Right column shows  $K_s$  against changing input water quality, which could be either salinity or sodicity. Input water quality changes such that degradation is more likely (i.e., salinity declines or sodium adsorption ratio (SAR) increases) as the axis moves to the right. Right column emphasizes how two weight functions can produce same degradation curve, but different rehabilitation patterns. Values for rehabilitation and degradation indices, respectively: A1 = (0.23, 0.15), A2 = (0.92, 0.15), B1 = (0.54, 0.44), B2 = (0.92, 0.44), C1 = (0.69, 0.68), C2 = (0.93, 0.68).

### 2.3. Effect of Weight Functions on Hysteresis Curves

The weight functions used in this paper are designed to emphasize contrasts in degradation and rehabilitation patterns. To facilitate quantitative comparison of soils, Adeyemo et al. (2022) and Kramer et al. (2021) developed degradation and rehabilitation indices, respectively. The degradation index is zero for no susceptibility to degradation, and one for maximal susceptibility. The rehabilitation index is zero for soils that show no  $K_s$  rehabilitation, and one for soils whose rehabilitation curves are exactly the same as their degradation curves, that is, when there is no  $K_s$  hysteresis to speak of. The left-hand side of Figure 1 shows representative 2D slices for the six weight functions used in the simulations that follow, positioned according to their degradation and rehabilitation index values. (Note. Complete weight functions consist of two 3D arrays—one for each input variable—as explained in Text S1 in Supporting Information S1, which also discusses our methodology for developing the weight functions).

In the Preisach framework, degradation is governed by the horizontal distribution of weights in the weight triangles. In Figure 1, weight functions with high degradation indices (C1, C2) have heavier weights on the right. Weight functions with lower degradation indices (A1, A2) have heavier weights on the left. The effect of this contrast is evident in the right-hand column of Figure 1, which shows how  $K_s$  changes with input for each of the respective weight functions. (Input in this case could be salinity or sodicity, the mechanism is the same.) The initial slope of the degradation curve is steepest when the degradation index is highest. When the degradation index is low,  $K_s$  is resistant to decline and the initial slope of the degradation curve (dotted lines) is less sharp.

Weights with the same degradation index produce the same degradation curve because they have the same horizontal weight distribution. While the hysteresis curves in this figure show full rehabilitation, the weight functions themselves can easily be modified so that only partial recovery is possible.

To underscore the importance of hysteresis, the weight functions were chosen such that they have different rehabilitation indices. In the Preisach framework, propensity to rehabilitate is dependent on the vertical distribution of the weights in the weight triangles. Visually, when the rehabilitation index is high, then the gap between the rehabilitation and degradation curves (in the right-hand column) is smallest. In Figure 1, the rehabilitation curves, based on the weight functions with low rehabilitation indices (solid lines) are further from the degradation curves than the rehabilitation curves based on weights functions with high reversibility indices (dashed lines). Actual weight functions are likely to depend on numerous soil properties, with clay content and specific clay mineralogy being particularly important.

At this point it is important to emphasize: while Figure 1 can aid our understanding of the connection between weight functions and hysteresis curves, weight functions alone tell us nothing about the rate at which  $K_s$  changes. That is, while weight functions are used to calculate  $K_s$  given a history of salinity and sodicity, the rest of the SOTE model is necessary in order to calculate these very input values. Understanding how evolving salinity and sodicity dynamics, as determined by SOTE, interact with the weight functions to drive changes in  $K_s$  over time, is our goal in the following sections.

#### 2.4. Remarks on Climate and Soil Parameters

Before moving to the simulations, we briefly discuss the climate and soil parameters required to run SOTE. The overall framework reflects this paper's goal of demonstrating how hysteresis impacts our assessment of degradation and rehabilitation patterns when irrigating with saline and sodic TWw. Use of saline and sodic TWw is especially common in water-scarce areas, where rainfall is typically seasonal. As such, in the simulations that follow, rainfall is restricted to a fraction of the year, with irrigation water applied in the remainder. Irrigation water is applied at a rate proportional to 110% of the maximal daily evapotranspiration rate (Ben-Gal et al., 2009; Ben-Gal & Shani, 2002), which is itself designed to vary seasonally according to a sinusoidal curve. The heights of precipitation events are determined based on a Weibull distribution. The Weibull distribution has two parameters,  $\lambda$  and  $k$ , which can be fit using rainfall records from a given location. A more detailed overview of the Weibull distribution is included in Text S2 in Supporting Information S1. We use parameters based on the Northern Negev region of Israel in our simulations. This area features a typical semiarid climate, receiving approximately 200 mm rain/year. The length of the average winter rainy season is about 130 days/year, with some rainfall occurring on approximately 30% of those days. Agriculture production in the surrounding areas, as in most of Israel, is reliant on TWw and on winter rainfall to leach the accumulated salts.

SOTE also requires a number of parameters related to soil hydraulic, physical, and chemical exchange properties. The usage of these parameters is unchanged from SOTE 1.0 (Kramer & Mau, 2020). The values that we use are included in Text S3 in Supporting Information S1.

### 3. Results and Discussion

#### 3.1. History-Dependent Versus Memoryless $K_s$

To demonstrate how hysteresis can affect our understanding of soil degradation and rehabilitation when irrigating with TWw, we juxtapose simulations using the six different weight functions (history-dependent) against simulations without hysteresis (memoryless). To facilitate this comparison, we introduce a modified version of SOTE, in which changes to  $K_s$  are determined according to the previously mentioned McNeal (1968) model. The McNeal model is an apt benchmark because it has been frequently used for studying the effects of water chemistry on soils, particularly as the back-end of Hydrus's function for relative  $K_s$  (Šimůnek et al., 2013). The Hydrus software package has itself been frequently used as a tool to study the effects of salinity and sodicity, including reclamation of sodic soils (Reading et al., 2012; Shaygan et al., 2018; Suarez, 2001; Šimunek & Suarez, 1997).

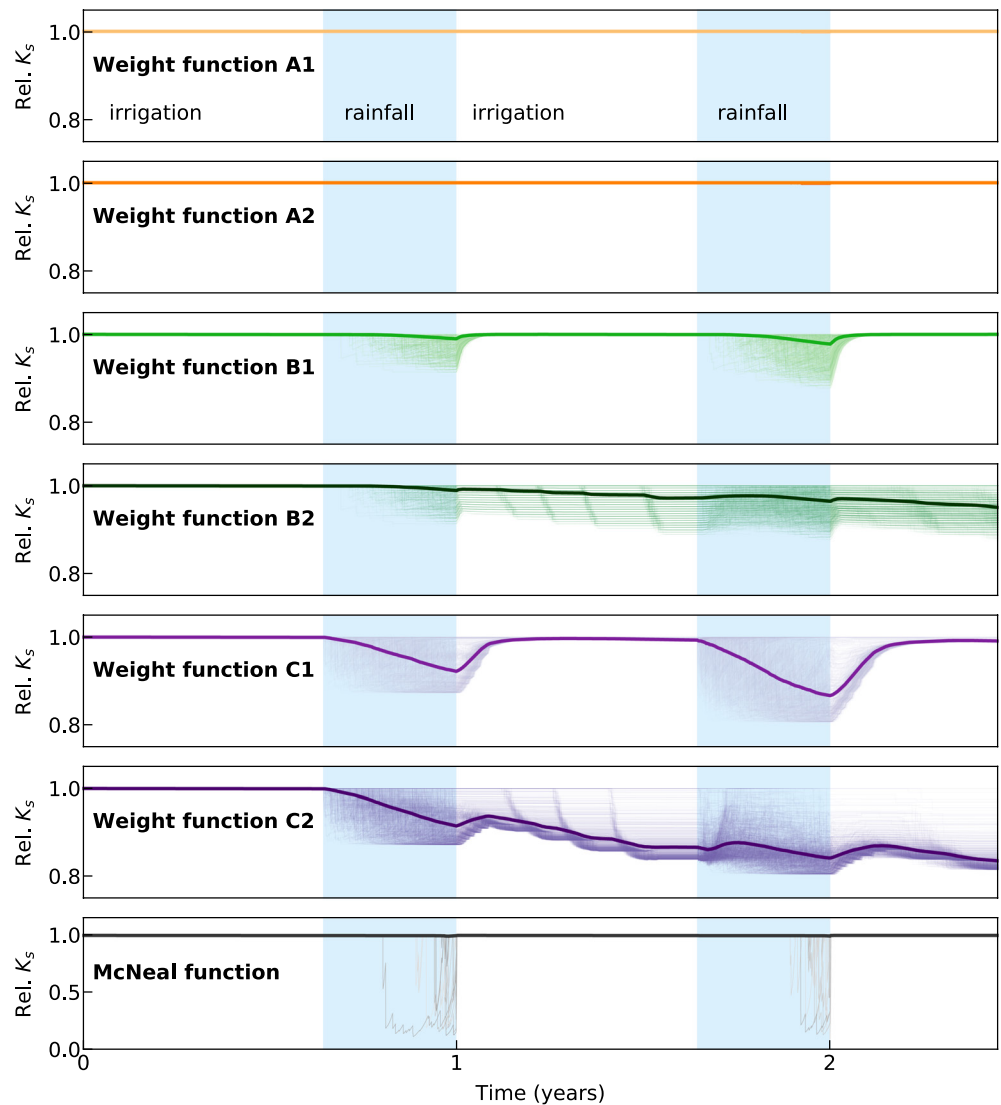


**Figure 2.** Degree of hysteresis changes the dynamics of soil degradation. Panels highlight 1,000 stochastic runs (thin lines) for each of the six different weight functions and the McNeal  $K_s$  function. The thick line in each panel shows the ensemble mean of the stochastic runs. The axis limits are different for panels (a–f) as compared to panel (g) because of the different scale of decline in relative  $K_s$  when using the McNeal function. Irrigation water quality:  $C_i = 15 \text{ mmol}_c \text{ L}^{-1}$  and  $E_i = 0.5$  (SAR = 3.9). Other parameters listed in Text S4 in Supporting Information S1.

### 3.1.1. Effect of Hysteresis on Degradation Risk

Focusing first on degradation, Figure 2 exemplifies how history-dependent  $K_s$  functions impact our understanding of the risk posed by a particular irrigation regime. The top six panels show changes in relative  $K_s$  for the six different weight functions; the bottom panel shows results based on the McNeal function. We define relative  $K_s$  as the current value of  $K_s$  as a fraction of its original value, with lower values indicating more severe degradation. The simulations themselves were run for 10.5 years, but we begin by focusing on the first two and a half years. The thin lines in each panel are the 1,000 stochastic runs used for each  $K_s$  function, each line with different stochastic precipitation series; the thicker lines are the ensemble means.

In a pattern typical of water-scarce regions, the irrigation water applied during the dry portion of the year (white shading) is saline ( $C_i = 15 \text{ mmol}_c \text{ L}^{-1}$ ) and heavily sodic ( $E = 0.5$ , SAR = 3.9). During the rainy season (blue shading), precipitation is assumed to be chemically neutral. This seasonal variation in input water quality leads to conditions of low salinity, but elevated sodicity, during the latter part of the rainy season (see Text S4 in

Supporting Information S1). When these conditions are particularly extreme and/or the weight function used is more susceptible to degradation, relative  $K_s$  declines. The degree of degradation corresponds to the distribution of weights, as discussed in Section 2.3. Weight functions A1 and A2 are highly resistant to declines in relative  $K_s$ , and therefore we see no serious degradation events in these simulations.

While seasonal degradation in relative  $K_s$  is more evident for weight functions B1, B2, C1, C2, and the McNeal function, there are major differences in how the runs in each simulation respond afterward. In the McNeal-based runs, which are not history-dependent, all declines in relative  $K_s$  are immediately reversed at the start of each new irrigation season. The hysteresis-based SOTE runs, however, vary in the speed and degree to which relative  $K_s$  rises following degradation events. The salinity and sodicity dynamics that drive these changes are consistent across the different simulations: the reintroduction of TWW at the end of each rainy season leads to sharp rises in salinity ( $C_s$ ), while the sodicity fraction ( $E_x$ ) changes at a much slower rate (Mau & Porporato, 2015). The McNeal model responds with immediate increases in relative  $K_s$ , while the other simulations do not, simply because the McNeal model is memoryless. It knows only that the new values of soil water salinity and sodicity would not lead to degradation if the soil were in its initial state, and therefore the value of relative  $K_s$  increases, regardless of the fact that soil is now starting from a degraded state. The weight functions, by contrast, are explicitly constrained by past salinity and sodicity conditions. What's more, the weight functions have built-in knowledge of a particular soil's propensity to rehabilitation, and can therefore require more (or less) sustained changes in input water chemistry to drive a rise in relative  $K_s$ .

The effect that hysteresis has on the results is more clearly understood by examining the differences between the SOTE simulations themselves. As described in Section 2.3, the weight functions are grouped in pairs, such that A1 and A2 have the same susceptibility to degradation, as do B1 and B2, and the same for C1 and C2. And while the members of each pair indeed exhibit the same initial degradation, their trajectories diverge following the end of the first rainy season, due to the fact that the weight functions in each pair differ in their propensity to rehabilitation. Weight functions B1 and C1, have higher rehabilitation indices, making it possible for relative  $K_s$  to rise quickly whenever saline TWW is reintroduced. On the other hand, recovery is delayed, or never occurs, when the simulations are run with weight functions B2 and C2, which have lower rehabilitation indices. The point here is simple but important: when hysteresis is included, soils will exhibit a range of responses following degradation events.

Bringing the question back to risk: assessments of the sustainability of irrigation with TWW would reach very different conclusions, depending on whether they used a history-dependent or memoryless model. Panels (a–c) in Figure 3 show probability density functions (PDFs) of the  $K_s$  values at the end of the 10.5-year simulation period, roughly in the middle of the dry season. (Results for weight functions A1 and A2 are omitted because no degradation was observed in these runs.) Panel (d) uses the same data to show the fraction of stochastic runs finishing under a particular  $K_s$  threshold, which we call the risk of long-term soil degradation. Because the McNeal-based model allows  $K_s$  to easily recover following degradation events, the results of this simulation show zero risk. Likewise, even though recovery takes slightly longer when using the weight functions with higher rehabilitation indices (B1 and C1), the PDFs for both are skewed to the right, and no run in these simulations finishes with a relative  $K_s$  value that is less than 0.95. When using weight functions B2 and C2, however, the situation is quite different. The PDFs are skewed to the left, and most runs finish with clear declines in relative  $K_s$ . When using weight function B2, the declines in relative  $K_s$  are moderate, with 36% of runs finishing with a relative  $K_s$  that is less than 0.9, but none with a relative  $K_s$  that is less than 0.80. When using weight function C2, more than 50% of runs finish with a relative  $K_s$  value that is less than 0.8.

These results raise an important point about the difference between risk and susceptibility. When analyzing the sustainability of TWW irrigation, it is tempting to presume that risk can be predicted based on initial susceptibility to degradation, that is, by the degradation index. The results presented here, however, make clear that susceptibility to degradation must be considered in tandem with propensity to rehabilitate. Inherent in the assumption that susceptibility to degradation provides the best indicator of risk is the expectation that soils with higher degradation indices are likely to have lower rehabilitation indices, and vice versa. Because of this, it is common to anticipate that soils are more likely to behave like those with weights B1 and C2 and less like B2 and C1. Lacking experimental evidence, however, this assumption does not have any foundation. In fact, initial experimental results indicate that in some cases soils with higher degradation indices also have higher rehabilitation indices (Adeyemo et al., 2022). Likewise, these results have shown that soils with lower degradation indices can

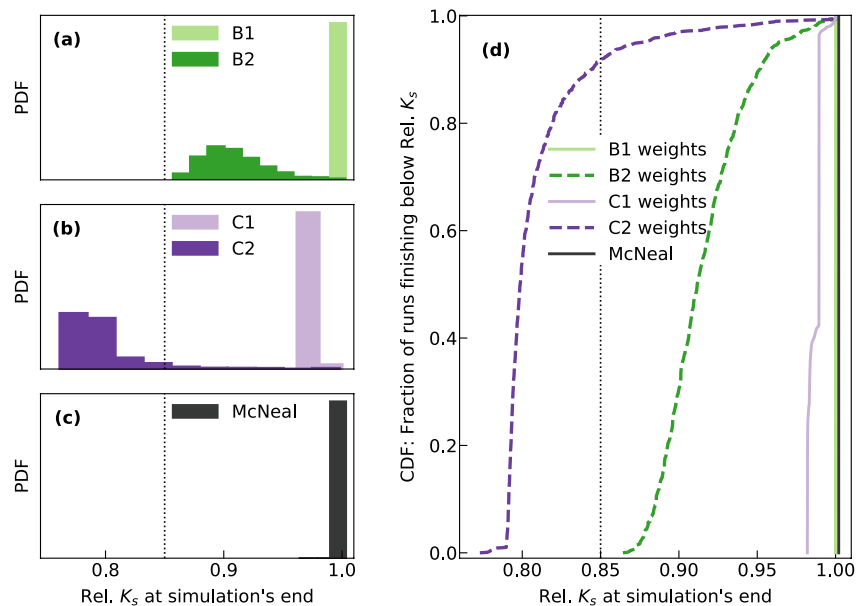


**Figure 3.** Risk of soil degradation changes based on which  $K_s$  function is used. Panels (a–c) show probability density functions of the relative  $K_s$  value at the end of the 10.5 years simulation. Panel (d) calculates cumulative distribution functions (CDFs) showing the fraction of runs finishing with a relative  $K_s$  value below a given threshold.

also be less likely to rehabilitate (Adeyemo et al., 2022). When this is the case, it is possible for soils with higher degradation indices (such as, C1) to have lower risk of long-term degradation than those with lower degradation indices (such as B2).

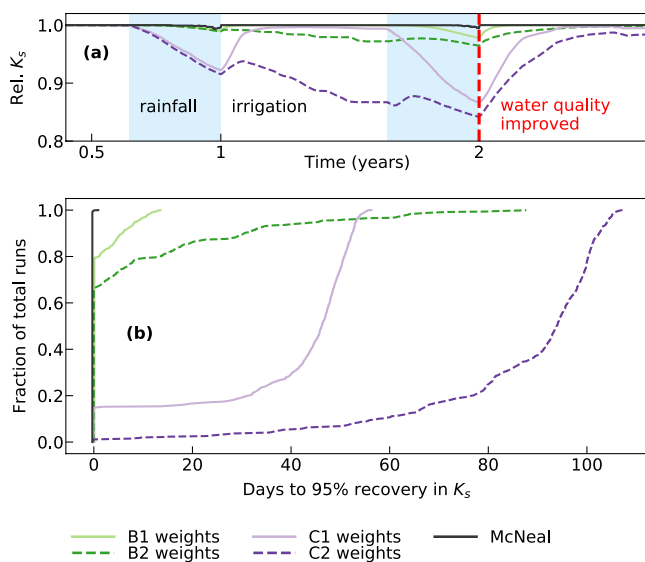


**Figure 4.** Estimates of rehabilitation time may be much longer when hysteresis is considered. Panel a shows ensemble mean based on 1,000 stochastic runs for three different  $K_s$  functions. Panel b shows time required for 95% of runs to return to their original  $K_s$  value, following application of higher quality irrigation water at the end of year two. Initial irrigation water quality:  $C_i = 15 \text{ mmol}_c \text{ L}^{-1}$  and  $E_i = 0.5$  (SAR = 3.9). New irrigation water quality:  $C_i = 10 \text{ mmol}_c \text{ L}^{-1}$  and  $E_i = 0.1$  (SAR = 0.5).

While it is not directly related to hysteresis, it is also important to note that the McNeal-based simulations are unique in the magnitude of their degradation events. In the history-dependent runs, relative  $K_s$  never dips below 0.75. When using the McNeal function, however, the minimum observed relative  $K_s$  value is 0.08. That is, when using the McNeal model, it is possible for relative  $K_s$  to jump almost instantaneously from 1 to 0 and then back to 1. While this strange output is partly the result of the McNeal model being memoryless, it is also due to the McNeal model being sensitive to small changes in salinity and sodicity. Minute differences in either of these variables can cause some runs to experience large declines in  $K_s$ , while others experience no change. Altogether, this brings into question the suitability of using the McNeal model to assess the risk of soil degradation.

### 3.1.2. Effect of Hysteresis on Rehabilitation

Inclusion of hysteresis in models likewise influences expectations for the amount of time and resources required to rehabilitate a degraded soil. This can be seen in Figure 4, which presents results based on a set of simulations in which (as in the simulations in the previous section), saline-sodic TWw was applied seasonally, with rainfall triggering declines in  $K_s$ . After 2 years, however, the quality of the irrigation water was improved: the relative concentration of sodium in the irrigation water was significantly lowered, in order to stimulate rehabilitation of  $K_s$ . As in the previous set of simulations, an ensemble of 1,000 stochastic runs was used for each of the  $K_s$  functions. Figure 4a shows the ensemble mean for weight functions B1, B2, C1, C2, and the McNeal  $K_s$  function during the simulation period. Figure 4b gives the amount of time required after the change in irrigation water chemistry

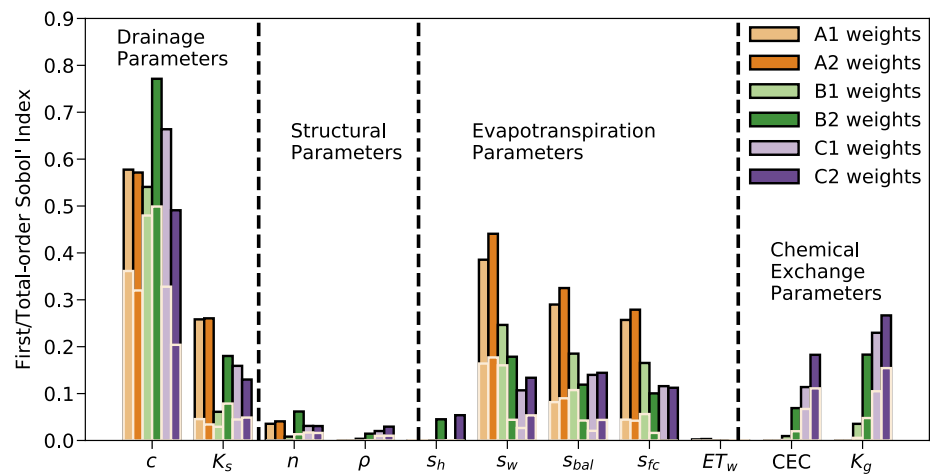


**Figure 5.** Sensitivity analysis demonstrates that drainage parameters accounts for largest proportion of variance in SOTE output. Figure shows First-order and Total-order Sobol' Indices for soil parameters used when running SOTE. Height of bars with white edges corresponds to first-order index. Height of bars with black edges corresponds to total-order index.

for relative  $K_s$  to return to 95% of its original value. Results from weight functions A1 and A2 are not displayed because of the minimal degradation observed in these simulations.

As in the previous set of simulations, the McNeal-based runs exhibit almost immediate rehabilitation, while changes in relative  $K_s$  show more variation for the hysteresis-based simulations. When using weight function C1, for instance, 80% of the runs “rehabilitate” (i.e., return to 95% of the original  $K_s$  value) within 50 days. When using weight function C2, however, rehabilitation is much slower: over 100 days are required for 80% of runs to rehabilitate, despite the fact that C1 and C2 undergo the same level of degradation. The contrast is less dramatic but still clear for weight functions B1 and B2. When using weight function B1, 80% of runs recover within a single day; for B2, 13 days are required. These differences in time, of course, directly correspond to differences in resources (i.e., water, chemical amendments) required in order to promote rehabilitation.

### 3.2. Variance-Based Sensitivity Analysis

In this section, we examine how uncertainty in the input parameters can affect SOTE's output. We do this by performing a Sobol' sensitivity analysis (Saltelli, 2002; Saltelli et al., 2010; Sobol, 2001) using SALib, an open-source Python library (Herman & Usher, 2017). We focus on the 11 parameters related to drainage, chemical exchange, evapotranspiration, and soil structure, generating 1,000 samples for each, within the bounds listed in Text S3 in Supporting Information S1 (24,000 total simulations). Parameters related to climate and irrigation were held constant during the sensitivity analysis, because varying them would have obscured our ability to understand the role of the soil parameters, about which there is likely to be much greater uncertainty. The results presented in this section are based on irrigation with saline-sodic water ( $C_i = 20 \text{ mmol}_c \text{ L}^{-1}$ ,  $E_i = 0.35$ ,  $\text{SAR} = 2.7$ ) and the climate parameters used in Section 2.4. To demonstrate that our results are not specific to these irrigation and climate parameters, we repeat the sensitivity analysis using different climate and irrigation regimes in Text S5 in Supporting Information S1. The simulations used in the sensitivity analysis followed a framework similar to that in Section 3.1.1: for each combination of parameters we ran a 1-year SOTE simulation, using 100 stochastic repetitions. We repeated this process for each of the six weight functions. In the analysis that follows, we focus on mean relative  $K_s$  as the output variable.

The sensitivity analysis indicates that the drainage and chemical exchange processes exert the most influence over relative  $K_s$ . SOTE computes drainage with a commonly used power function for unsaturated hydraulic conductivity,  $K_{s,s^c}$ , where  $s$  is the relative soil moisture content and the exponent  $c$  can be linked to Brook and Corey's pore size distribution index,  $\lambda$  (Assouline & Or, 2013). The importance of the drainage parameters is evident in Figure 5, which shows the First-Order and Total-Order Sobol' Indices for each parameter. These indices give the fraction of the total variance accounted for by each parameter, excluding (first-order) and including (total-order) interactions with all other parameters. The indices show that drainage parameters account for the largest fraction

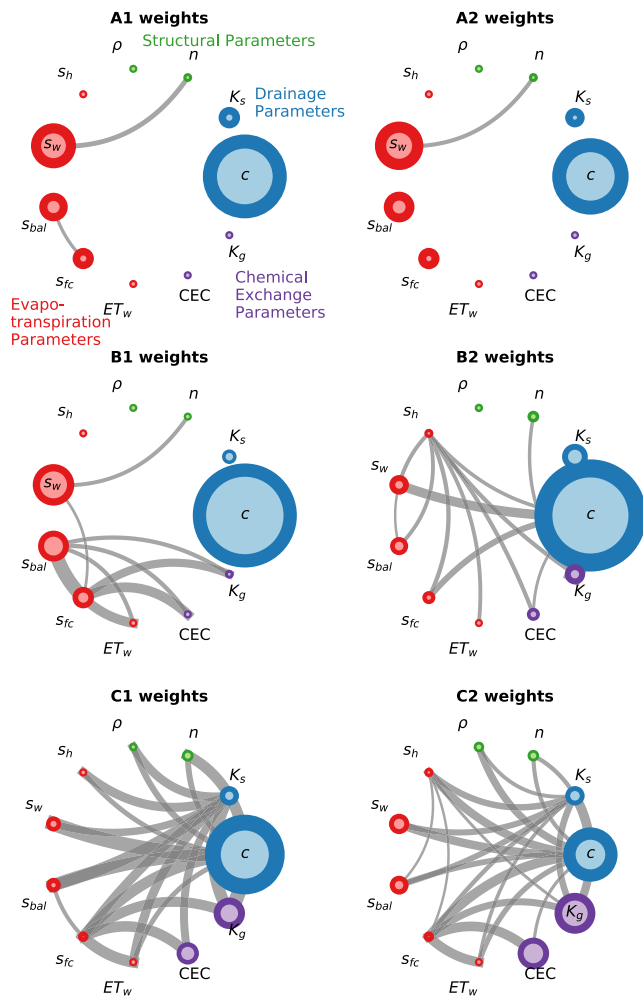


**Figure 6.** Sensitivity analysis results also indicate that drainage parameters have the most interactions with other parameters. The radius of lightly shaded circles corresponds to the first-order index, while the radius of the light and dark circles together corresponds to the total-order index. The difference between the total- and first-order indices corresponds to interactions between different parameters, and the width of the lines between parameters represents the relative size of the second-order interactions between a specific pair of parameters.

of total variance, regardless of which weight function is used. The parameter  $c$  has much larger index values than  $K_s$ , but this is because  $c$  appears in the exponent of the drainage equation, and therefore we analyze these parameters as a group, since they collectively determine the drainage rate. The high influence that the drainage rate exerts on the results makes sense, because drainage is the primary mechanism for salt removal, and therefore determines the rate at which salts exit the root zone. Degradation is most likely when the salinity concentration drops quickly, while the sodicity fraction remains elevated, so it is not surprising that the parameters that control drainage have a large influence on relative  $K_s$ .

The results in Figure 5 also demonstrate that the chemical exchange processes become increasingly important as susceptibility to degradation increases. When using weights A1 and A2, which are the most resistant to initial degradation, chemical exchange accounts for almost none of the total variance. Because these weight functions experience little degradation even when sodicity conditions are severe, it is understandable that the chemical exchange processes exert little effect on relative  $K_s$ . Likewise, it makes sense that the fraction of the variance accounted for by the chemical exchange properties rises, when we use weight functions B1, B2, C1, and C2. These weight functions allow for degradation at lower sodicity levels, and therefore the parameters that control the actual sodicity levels begin to exert more influence over the results.

These results make clear that practitioners should pay careful attention to the drainage and chemical exchange properties of soils when using SOTE as a forecasting tool. Other parameters, it can be noted, account for only minimal levels of variance. Varying the value of the structural parameters and evapotranspiration parameters leads to minimal changes in SOTE's output, suggesting that these parameters can be fixed without materially affecting the model's results.

The results also show that the drainage parameters have the most interactions with other parameters and that interactions between parameters increase as susceptibility to degradation increases. This can be seen in Figure 6, in which radial convergence plots show the pairwise interactions between parameters. In this figure, the lines connecting the parameters represent interactions, with the width of the line scaled to reflect the relative fraction of the variance accounted for by the interaction. When using weights with low degradation indices (A1, A2), few meaningful pairwise interactions are seen between the parameters. As initial susceptibility to degradation increases, however, pairwise interactions become more numerous. The parameters  $c$  and then  $K_s$  become hubs of interaction, again emphasizing the importance of the drainage process to changes in  $K_s$ . Compared to weights B1 and C1, we also note that B2 and C2 exhibit more interactions. We believe this reflects the overall higher level of variation in relative  $K_s$  when using B2 and C2, and does not offer any worthwhile insight into the model's behavior. It is also important to note that overall fraction of the variance accounted for by the interactions is much lower than that accounted for by the first-order indices.

Importantly, the Sobol' analysis can also be used to identify parameter ranges that are most likely to cause significant declines in relative  $K_s$ . Figure 7 focuses on the four parameters with the highest Sobol' Indices, mapping how their variation affects SOTE's output. Taking  $c$  as a first example, Figure 7 shows that low values of  $c$ , which are associated with higher leakage rates, cause the most variation in relative  $K_s$ . This is consistent with the argument that declines in relative  $K_s$  are most likely when salinity drops quickly, as can occur when a soil is fast draining. Likewise, higher values of the Gapon coefficient ( $K_d$ ), which is related to the exchange of cations between soil particles and the soil water, cause more variation in relative  $K_s$ . It is also clear, however, that the results are highly dependent on which weight function is used. When using weight functions A1 and A2, relative  $K_s$  is confined to

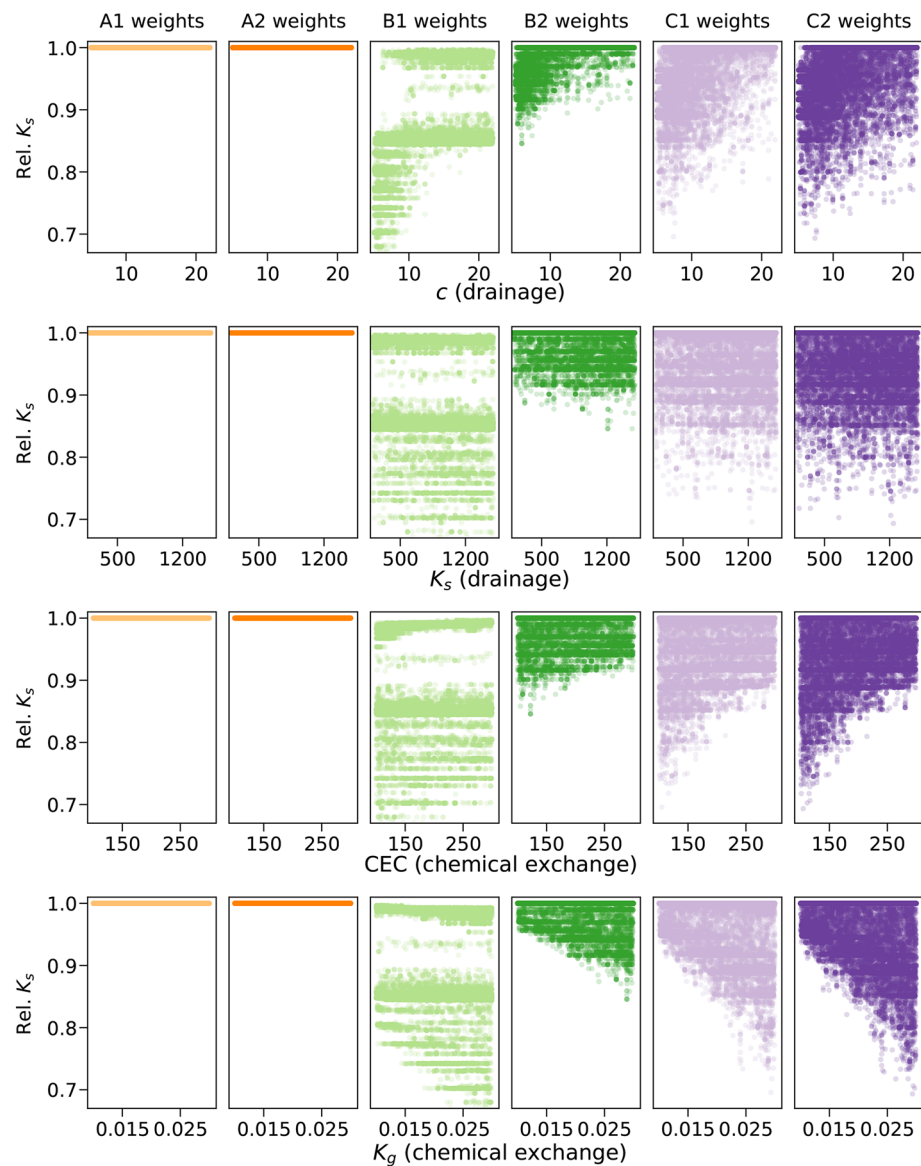


**Figure 7.** Sensitivity analysis results can be used to identify parameter ranges that cause the largest variation in relative  $K_s$  results. Output for each combination of parameters used in sensitivity analysis is plotted against range of values for a specific parameter, for all 24,000 simulations.

a very narrow range, regardless of which parameter values are used. When using weight functions C1 and C2, by contrast, there is much higher degree or variance in relative  $K_s$  values. Figure 7 thus represents a useful complement to the results in Figures 5 and 6. While Figures 5 and 6 are helpful in understanding the fraction of variance accounted for by each parameter, they do not provide any information about how much variance there is in relative  $K_s$  itself. When evaluating the importance of the different parameters, it is important that we consider both of these factors together. In the future, we can also use this same approach to determine which climate regimes and irrigation strategies are most likely to cause declines in relative  $K_s$ .

#### 4. Conclusions

This paper's goal was to demonstrate the importance of hysteresis in  $K_s$  when evaluating the sustainability of irrigation with saline and sodic treated wastewater. While the examples presented are theoretical, SOTE simulations illustrate that hysteresis is essential to understanding both the degradation and rehabilitation processes.

When hysteresis is not taken into account, it is likely that models for the effect of irrigation with TWW are overly optimistic—underestimating the risk of long-term degradation and the cost of rehabilitation. Similar results are likely to be achieved when modeling irrigation with other marginal quality water resources, such as brackish groundwater.

Initial experimental results have supported the hypothesis that changes in  $K_s$  are characterized by hysteresis and the SOTE simulations presented here underscore the need for additional experimental work on this question. The weight functions that we used were synthetic—designed to demonstrate a range of possible soil behaviors. Only with more detailed experimental studies can we increase our understanding of the extent to which different soils experience actual hysteresis in  $K_s$ . The SOTE simulations do make clear, however, that differences in degree of hysteresis can have profound effects on degradation risk. That is, when trying to quantify the probability of long-term degradation, knowledge of a soil's propensity to rehabilitation (as measured by the rehabilitation index) is just as crucial as knowing its susceptibility to degradation (degradation index).

In this paper, we focused on degradation risk as a result of TWW, but future research should consider degradation risk in tandem with salinity hazards. The sensitivity analysis emphasized the importance of drainage to degradation risk, with degradation most likely when soil salinity quickly drops and sodicity remains elevated. Avoiding degradation at the cost of increasing salinity would miss the point, however, if the salinity level is too high for plant growth. Likewise, while leaching the root zone can be effective in the short-term, drainage is costly and potentially harmful, if it causes a rise in the water table or pollutes groundwater resources. In order for irrigation with marginal quality water to be truly sustainable, we must find strategies that minimize degradation risk while also addressing these other concerns.

While SOTE's results must make us cautious about the sustainability of TWW irrigation, they also present an opportunity. That is, increased knowledge of the risk that irrigation with TWW poses does not mean we need to abandon the practice. Rather, models that better reflect actual risk are considered a priority for research on salinity because they can allow for more effective management (Hopmans et al., 2021). In other words, better understanding of the risks associated with TWW can enable more responsible use of saline and sodic waters, allowing for their continued use in ways that also minimize the probability of long-term damage to soils.

## Data Availability Statement

Code used to run the SOTE 2.0 model is available at <https://github.com/isaackramer/SOTE-2.0>.

## Acknowledgments

We thank Guy Levy and Efrat Morin for useful discussion. We thank Antonia Hadjimichael for sharing her code on how to produce radial converge plots, on the Water Programming blog (<https://waterprogramming.wordpress.com/>). We thank Jon Herman for his support with using SALib. We thank R. W. Vervoort for his constructive suggestions during review, and for his continuing support and insightful discussion.

## References

- Adeyemo, T., Kramer, I., Levy, G. J., & Mau, Y. (2022). Salinity and sodicity can cause hysteresis in soil hydraulic conductivity. *Geoderma*, 413(2), 15765. <https://doi.org/10.1016/j.geoderma.2022.115765>
- Assouline, S., & Narkis, K. (2011). Effects of long-term irrigation with treated wastewater on the hydraulic properties of a clayey soil. *Water Resources Research*, 47, W08530. <https://doi.org/10.1029/2011WR010498>
- Assouline, S., & Narkis, K. (2013). Effect of long-term irrigation with treated wastewater on the root zone environment. *Vadose Zone Journal*, 12(2), vzj2012.0216. <https://doi.org/10.2136/vzj2012.0216>
- Assouline, S., & Or, D. (2013). Conceptual and parametric representation of soil hydraulic properties: A review. *Vadose Zone Journal*, 12(4), vzj2013.07. <https://doi.org/10.2136/vzj2013.07.0121>
- Assouline, S., Russo, D., Silber, A., & Or, D. (2015). Balancing water scarcity and quality for sustainable irrigated agriculture. *Water Resources Research*, 51, 3419–3436. <https://doi.org/10.1002/2015WR017071>
- Bardhan, G., Russo, D., Goldstein, D., & Levy, G. J. (2016). Changes in the hydraulic properties of a clay soil under long-term irrigation with treated wastewater. *Geoderma*, 264, 1–9. <https://doi.org/10.1016/j.geoderma.2015.10.004>
- Ben-Gal, A., Agam, N., Alchanatis, V., Cohen, Y., Yermiyahu, U., Zipori, I., et al. (2009). Evaluating water stress in irrigated olives: Correlation of soil water status, tree water status, and thermal imagery. *Irrigation Science*, 27, 367–376. <https://doi.org/10.1007/s00271-009-0150-7>
- Ben-Gal, A., & Shani, U. (2002). Yield, transpiration and growth of tomatoes under combined excess boron and salinity stress. *Plant and Soil*, 247, 211–221. <https://doi.org/10.1023/A:1021556808595>
- Ben-Gal, A., Tal, A., & Tel-Zur, N. (2006). The sustainability of arid agriculture: Trends and challenges. *Annals of Arid Zone*, 45(2), 1–31.
- Bixio, D., Thoeue, C., De Koning, J., Joksimovic, D., Savic, D., Wintgens, T., et al. (2006). Wastewater reuse in Europe. *Desalination*, 187, 89–101. <https://doi.org/10.1016/j.desal.2005.04.070>
- Bolt, G. H. (1967). Cation-exchange equations used in soil science: A review. *Netherlands Journal of Agricultural Science*, 15, 81–103. <https://doi.org/10.18174/njas.v15i2.17442>
- Bresler, E., McNeal, B. L., & Carter, D. L. (1982). *Saline and sodic soils: Principles-dynamics-modeling* (Vol. 10). Springer-Verlag. <https://doi.org/10.1007/978-3-642-68324-4>
- Dane, J. H., & Klute, A. (1977). Salt effects on the hydraulic properties of a swelling soil. *Soil Science Society of America Journal*, 41, 1043–1049. <https://doi.org/10.2136/sssaj1977.03615995004100060005x>

- Dery, J. L., Rock, C. M., Goldstein, R. R., Onumajuru, C., Brassill, N., Zozaya, S., et al. (2019). Understanding grower perceptions and attitudes on the use of nontraditional water sources, including reclaimed or recycled water, in the semi-arid Southwest United States. *Environmental Research*, *170*, 500–509. <https://doi.org/10.1016/j.envres.2018.12.039>
- Dregne, H. E., & Chou, N. (1992). Global desertification dimensions and costs. In *Degradation and restoration of arid lands*. Texas Tech. University.
- Ezlit, Y. D., Bennett, J. M., Raine, S. R., & Smith, R. J. (2013). Modification of the McNeal clay swelling model improves prediction of saturated hydraulic conductivity as a function of applied water quality. *Soil Science Society of America Journal*, *77*, 2149–2156. <https://doi.org/10.2136/sssaj2013.03.0097>
- Gharaibeh, M. A., Eltaif, N., & Albalasmeh, A. (2011). Reclamation of highly calcareous saline sodic soil using Atriplex Halimus and by-product gypsum. *International Journal of Phytoremediation*, *13*, 873–883. <https://doi.org/10.1080/15226514.2011.573821>
- Herman, J., & Usher, W. (2017). SALib: An open-source python library for sensitivity analysis. *The Journal of Open Source Software*, *2*, 97. <https://doi.org/10.21105/joss.00097>
- Hillel, D. (1998). *Environmental soil physics*. Academic Press.
- Hillel, D. (2000). *Salinity management for sustainable irrigation: Integrating science, environment, and economics* (Tech. Rep.). The World Bank.
- Hopmans, J. W., Qureshi, A. S., Kisekka, I., Munns, R., Grattan, S. R., Rengasamy, P., et al. (2021). Critical knowledge gaps and research priorities in global soil salinity. *Advances in Agronomy*, *169*, 1–191. <https://doi.org/10.1016/bs.agron.2021.03.001>
- Jaramillo, M., & Restrepo, I. (2017). Wastewater reuse in agriculture: A review about its limitations and benefits. *Sustainability*, *9*, 1734. <https://doi.org/10.3390/su9101734>
- Kramer, I., Bayer, Y., Adeyemo, T., & Mau, Y. (2021). Hysteresis in soil hydraulic conductivity as driven by salinity and sodicity—A modeling framework. *Hydrology and Earth System Sciences*, *25*, 1993–2008. <https://doi.org/10.5194/hess-2020-455>
- Kramer, I., & Mau, Y. (2020). Soil degradation risks assessed by the SOTE model for salinity and sodicity. *Water Resources Research*, *56*, e2020WR027456. <https://doi.org/10.1029/2020WR027456>
- Läuchli, A., & Grattan, S. R. (2011). Plant responses to saline and sodic conditions. In W. W. Wallender & K. K. Tanji (Eds.), *Agricultural salinity assessment and management* (pp. 169–205). American Society of Civil Engineers. <https://doi.org/10.1061/9780784411698.ch06>
- Levy, G. J., Goldstein, D., & Mamedov, A. I. (2005). Saturated hydraulic conductivity of semiarid soils: Combined effects of salinity, sodicity, and rate of wetting. *Soil Science Society of America Journal*, *69*, 653–662. <https://doi.org/10.2136/sssaj2004.0232>
- Mau, Y., & Porporato, A. (2015). A dynamical system approach to soil salinity and sodicity. *Advances in Water Resources*, *83*, 68–76. <https://doi.org/10.1016/j.advwatres.2015.05.010>
- McNeal, B. L. (1968). Prediction of the effect of mixed-salt solutions on soil hydraulic conductivity. *Soil Science Society of America Journal*, *32*, 190–193. <https://doi.org/10.2136/sssaj1968.03615995003200020013x>
- McNeal, B. L., & Coleman, N. T. (1966). Effect of solution composition on soil hydraulic conductivity. *Soil Science Society of America Journal*, *30*, 308–312. <https://doi.org/10.2136/sssaj1966.03615995003000030007x>
- Olsson, L., Barbosa, H., Bhadwal, S., Cowie, A., Delusca, K., Flores-Renteria, D., & Stringer, L. (2019). Land degradation. In P. Shukla, J. Skea, E. Calvo Buendia, V. Masson-Delmotte, H.-O. Pörtner, D. C. Roberts, et al. (Eds.), *Climate change and land: An IPCC special report on climate change, desertification, land degradation, sustainable land management, food security, and greenhouse gas fluxes in terrestrial ecosystems* (pp. 345–436). IPCC.
- Oster, J. D. (1993). Sodic soil reclamation. In H. Lieth, & A. A. Al Masoom (Eds.), *Towards the rational use of high salinity tolerant plants. Tasks for vegetation science*. Springer. [https://doi.org/10.1007/978-94-011-1858-3\\_51](https://doi.org/10.1007/978-94-011-1858-3_51)
- Práválie, R., Patriche, C., Borrelli, P., Panagos, P., Ro ca, B., Dumitrascu, M., et al. (2021). Arable lands under the pressure of multiple land degradation processes. A global perspective. *Environmental Research*, *194*, 110697. <https://doi.org/10.1016/j.envres.2020.110697>
- Qadir, M., Schubert, S., Ghafoor, A., & Murtaza, G. (2001). Amelioration strategies for sodic soils: A review. *Land Degradation & Development*, *12*, 357–386. <https://doi.org/10.1002/ldr.458>
- Reading, L. P., Baumgartl, T., Bristow, K. L., & Lockington, D. A. (2012). Applying HYDRUS to flow in a sodic clay soil with solution composition-dependent hydraulic conductivity. *Vadose Zone Journal*, *11*(2), vzj2011.0137. <https://doi.org/10.2136/vzj2011.0137>
- Safriel, U., Adeel, Z., Niemeijer, D., Puigdefabregas, J., White, R., Lal, R., & McNab, D. (2005). Dryland systems. In R. Hassan, R. Scholes, & N. Ash (Eds.), *Ecosystems and human well-being: Current state and trends* (Vol. 1, pp. 623–662). Island Press.
- Saltelli, A. (2002). Making best use of model evaluations to compute sensitivity indices. *Computer Physics Communications*, *145*, 280–297. [https://doi.org/10.1016/S0010-4655\(02\)00280-1](https://doi.org/10.1016/S0010-4655(02)00280-1)
- Saltelli, A., Annoni, P., Azzini, I., Campolongo, F., Ratto, M., & Tarantola, S. (2010). Variance based sensitivity analysis of model output. Design and estimator for the total sensitivity index. *Computer Physics Communications*, *181*, 259–270. <https://doi.org/10.1016/j.cpc.2009.09.018>
- Shainberg, I., & Letey, J. (1984). *Response of soils to sodic and saline conditions* (Vol. 52). University of California Division of Agriculture and Natural Resources. <https://doi.org/10.3733/hilg.v52n02p057>
- Shainberg, I., & Levy, G. J. (1992). Physico-chemical effects of salts upon infiltration and water movement in soils. In *Interacting processes in soil science*. Lewis Publishers.
- Shainberg, I., & Singer, M. J. (2011). Soil response to saline and sodic conditions. In W. W. Wallender, & K. K. Tanji (Eds.), *Agricultural salinity assessment and management* (pp. 139–167). American Society of Civil Engineers. <https://doi.org/10.1061/9780784411698.ch05>
- Shaygan, M., Baumgartl, T., Arnold, S., & Reading, L. P. (2018). The effect of soil physical amendments on reclamation of a saline-sodic soil: Simulation of salt leaching using HYDRUS-1D. *Soil Research*, *56*, 829–845. <https://doi.org/10.1071/SR18047>
- Šimůnek, J., Sakai, M., Van Genuchten, M., Saito, H., & Sejna, M. (2013). *The HYDRUS-1D software package for simulating the one-dimensional movement of water, heat, and multiple solutes in variably-saturated media*. CSIRO.
- Šimůnek, J., & Suarez, D. L. (1997). Sodic soil reclamation using multicomponent transport modeling. *Journal of Irrigation and Drainage Engineering*, *123*, 367–376. [https://doi.org/10.1061/\(ASCE\)0733-9437\(1997\)123:5\(367\)](https://doi.org/10.1061/(ASCE)0733-9437(1997)123:5(367))
- Sobol, I. M. (2001). Global sensitivity indices for nonlinear mathematical models and their Monte Carlo estimates. *Mathematics and Computers in Simulation*, *55*, 271–280. [https://doi.org/10.1016/S0378-4754\(00\)00270-6](https://doi.org/10.1016/S0378-4754(00)00270-6)
- Suarez, D. L. (2001). Sodic soil reclamation: Modelling and field study. *Australian Journal of Soil Research*, *39*(6), 1225–1246. <https://doi.org/10.1071/SR00094>
- van der Zee, S., Shah, S., & Vervoort, R. (2014). Root zone salinity and sodicity under seasonal rainfall due to feedback of decreasing hydraulic conductivity. *Water Resources Research*, *50*, 9432–9446. <https://doi.org/10.1002/2013WR015208>
- Winpenny, J., Heinz, I., & Koo-Oshima, S. (2010). *The wealth of waste: The economics of wastewater use in agriculture* (Tech. Rep. No. 35). FAO.

- Yaron, B., & Thomas, G. W. (1968). Soil hydraulic conductivity as affected by sodic water. *Water Resources Research*, *4*, 545–552. <https://doi.org/10.1029/WR004i003p00545>
- Yin, X., Feng, Q., Li, Y., Liu, W., Zhu, M., Xu, G., et al. (2021). Induced soil degradation risks and plant responses by salinity and sodicity in intensive irrigated agro-ecosystems of seasonally-frozen arid regions. *Journal of Hydrology*, *603*, 127036. <https://doi.org/10.1016/j.jhydrol.2021.127036>

### References From the Supporting Information

- Abernethy, R. B. (2000). *The new Weibull handbook: Reliability & statistical analysis for predicting life, safety, survivability, risk, cost and warranty claims* (4th ed.). R.B. Abernethy.
- Laio, F., Porporato, A., Fernandez-Illescas, C., & Rodriguez-Iturbe, I. (2001). Plants in water-controlled ecosystems: Active role in hydrologic processes and response to water stress. *Advances in Water Resources*, *24*, 745–762. [https://doi.org/10.1016/S0309-1708\(01\)00007-0](https://doi.org/10.1016/S0309-1708(01)00007-0)
- Levy, R., & Muravsky, E. (1965). Soluble and exchangeable cation ratios in some soils of Israel. *Journal of Soil Science*, *16*, 290–295. <https://doi.org/10.1111/j.1365-2389.1965.tb01440.x>
- Richard, L. (Ed.). (1954). Diagnosis and improvement of saline and alkaline soils.